Research Article

Liuyang Bai*, Yuge Ouyang, Hongbing Wang, Min Wang, and Fangli Yuan*

Off-gas detection and treatment for green air-plasma process

Abstract: Thermal plasma is a promising technology widely used in materials processing and waste treatment due to its unique properties including high temperature, high energy density, high chemical activity, and high quench rate. Air-plasma is preferentially used because air is of low price as plasma gas. The content of NO_x in off-gas from air-plasma was determined using a gas analyzer, and a treatment unit was designed for the green air-plasma process. Results show that the concentration of NO_x in off-gas from air-plasma was 2,489 and 9,112 ppm when the plasma input power was 50 and 150 kW, respectively. O_2 in the off-gas would act as an oxidant to promote NO_x absorption; thus, alkali absorption method was directly used for the treatment of the present off-gas from air-plasma. The absorption efficiency could be increased to 62.2% when additional O_2 was provided into the off-gas to change its O_2 content from 20% to 50%. The absorption rate was estimated based on the experimental data and a multistage absorption unit design, which could be reduced below 100 ppm and meet the emission standard. This article presents the feasibility of thermal plasma off-gas purification, so as to truly realize the green plasma process.

Keywords: thermal plasma, off-gas, removal of NO_x, green process

* **Corresponding author: Liuyang Bai,** College of Energy Engineering, Huanghuai University, Zhumadian, 463800, China; State Key Laboratory of Multi-phase Complex Systems, Institute of Process Engineering, Chinese Academy of Sciences, Beijing 100190, China, e-mail: lybai@huanghuai.edu.cn
* **Corresponding author: Fangli Yuan,** State Key Laboratory of Multi-phase Complex Systems, Institute of Process Engineering, Chinese Academy of Sciences, Beijing 100190, China, e-mail: flyuan@ipe.ac.cn
Yuge Ouyang: College of Chemistry and Materials Engineering, Beijing Technology and Business University, Beijing, China
Hongbing Wang, Min Wang: Henan Huiqiang New Energy Material Technology Co., Ltd, Zhumadian, 463800, China

1 Introduction

Plasma is usually considered the fourth state of matter that is different from solid, liquid, and gaseous substances. It is a quasi-neutral gas composed of electrons, ions, neutrals in the ground state, excited species, and photons, in which the total number of positive charges is equal to that of negative charges [1,2]. Plasma can be mainly divided into high-temperature plasma and low-temperature plasma according to the ionization degree and temperature [3,4]. High-temperature plasma exhibits similar temperatures for electrons and ions and a very high ionization degree ($\approx$1), while low-temperature plasma exhibits higher electron temperature T_e and lower ion temperature T_i, in this case, a partially ionized medium [5]. Low-temperature plasma can be further classified as thermal and non-thermal plasma, where plasma with a comparable temperature of heavy ions to that of electrons is known as thermal plasma [6].

Thermal plasma is usually generated by way of making electric current pass-through gases. Many routes, such as direct current (DC), alternating current (AC), radio frequency (RF) and microwaves, have been employed to generate thermal plasma [7]. The plasma torch can be classified according to the generating source, calling DC plasma, AC plasma, and RF plasma. The DC arc plasma is usually used in two modes as non-transferred arc and transferred arc [8]. Thermal plasma has distinct properties compared to ordinary chemical reaction media, including high temperature, high energy density, and high chemical activity, which makes plasma a promising technology widely used in material processing and waste treatment, usually known as "plasma enhancement" [2,5].

Plasma processing of materials can be classified into four categories [9,10]. (i) Plasma spheroidization: powders with irregular shape fed into plasma flame were melted in the high-temperature region to form spherical liquid drops and then fast quenched (with sufficient water-cooling or gas-cooling out of the plasma flame) to form spherical powders under sharp quenching rate [11–13]. (ii) Thermal plasma evaporation and condensation: powders with large

sizes were fed into plasma flame and vaporized, and ultra-fine powders were produced after fast quenching by physical vapor deposition [14–16]. (iii) Plasma-enhanced chemical vapor deposition: reaction precursors are fed in the form of gases of vapors, and plasma is introduced into the reaction zone to activate the precursors [17–21]. (iv) Plasma treatment of solid phases: target material is prepared by simply exposing the solid precursor to plasma through plasma–solid interaction [22,23].

Thermal plasma is also successfully applied to treat a variety of wastes. On the one hand, plasma can thermally decompose hazardous organic compounds into simpler fuel gas which in turn was employed for diverse applications [24]. On the other hand, plasma also helps melt solid inorganic components or, with the addition of glass former, vitrify waste to form a stable glassy slag product in which hazardous substances are trapped within the glass network. The inert glassy slag which is obtained as a by-product in the plasma-assisted waste treatment can be upgraded to value-added products such as glass ceramics, road filler material, and building construction material [25,26]. Different waste types such as municipal wastes (paper, biomass, plastic, cloth, etc.) and hazardous wastes (from industrial, agriculture, and hospitals) were processed via thermal plasma technology [27–31].

In a project of thermal plasma processing, one of the main parameters which need to take into account is the system pressure. In principle, atmospheric-pressure plasma devices can provide a crucial advantage over low-pressure plasma because they eliminate complications introduced by the need for vacuum. Therefore, atmospheric pressure plasma has been mostly employed for material processing and waste treatment. Air is the most common gas used, but several inert gases (N_2, He, Ar, etc.) have also been widely used as plasma gas [32–34]. When air is used, it must be subjected to a large differential in electrical potential in order for air to conduct electricity. Otherwise, Ar is usually used at the initial stage of the arc ignition process and switched to air after the plasma operates stably.

Another problem with the use of air as a thermal plasma gas is that N_2 and O_2 would react with each other to form NO_x in the unordinary chemical reaction media provided by thermal plasma. When a plasma wind tunnel was used for ablation of ultrahigh temperature ceramic materials, there existed NO_x in the exhaust gas which could be preliminarily judged through the color and smell.

This article will discuss the exhaust gas treatment based on the data accumulation. The content of NO_x in off-gas from air-plasma was determined using a gas analyzer, removal methods and their important parameters were examined according to the characteristics of plasma off-gas, and a treatment unit was designed so as to truly realize the green plasma process.

2 Experimental

Different thermal plasma devices including DC plasma, RF plasma, and three-phase AC plasma were designed and used in our laboratory. The DC plasma and three-phase AC plasma are usually applied for waste treatment, and the RF plasma is commonly used for functional powder material synthesis. DC plasma is also used to test the ablation behavior of ultra-high-temperature materials. When the air was used as plasma gas during these processes, the off-gas was a light brown pungent gas. We supposed that something had to be conducted for the plasma technique both in experimental conduction and in future application.

Figure 1 illustrates the off-gas treatment unit connected with the thermal plasma reactor. The green lines exhibit the gas flow path, while the blue lines are the circulating absorption liquid pipeline. Air is supplied by the air compressor as the plasma gas, and the off-gas is exhausted by an air pump and sent into the off-gas treatment unit. The gas to be treated enters from the bottom of the absorption tower and runs upward, while the absorption liquid enters from the top of the absorption tower and runs downward driven by a circulating pump. In order to enhance their contact and absorption efficiency, we set up sieve plates and porous suspended ball fillers in the absorption tower. The gas before and after absorption was tested using a gas analyzer. The off-gas after absorption was exhausted to the atmosphere or introduced into a secondary stage absorption.

Figure 2 shows the pictures of off-gas treatment unit connected with RF (Figure 2a) and DC (Figure 2b) plasma reactor, respectively. Plasma is usually ignited using Ar as a working gas and switched to air afterward. The off-gas is pumped out of the plasma reactor so that the system pressure maintains at negative pressure, which is conducive to the stable operation of thermal plasma for a long time. In the present work, the plasma equipment runs without any materials treated, so that all NO_x comes from the plasma itself. The off-gas was tested online using a flue gas analyzer (Testo-350, Testoterm).
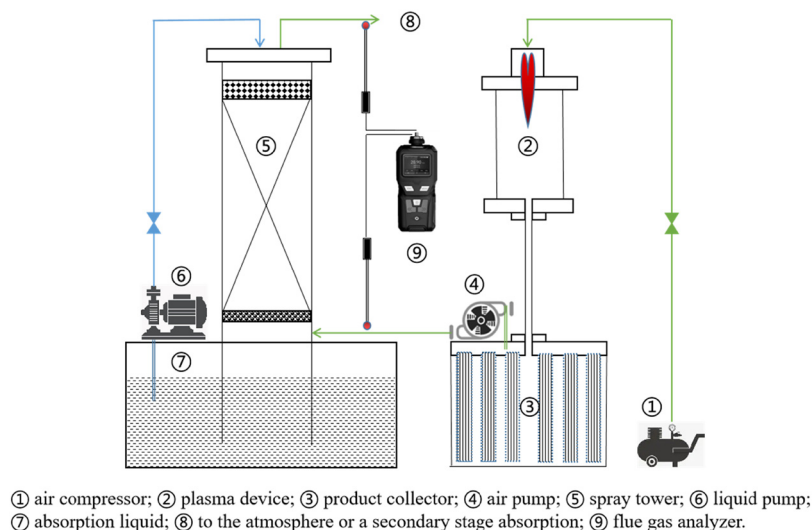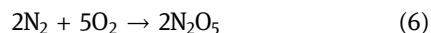
① air compressor; ② plasma device; ③ product collector; ④ air pump; ⑤ spray tower; ⑥ liquid pump;
⑦ absorption liquid; ⑧ to the atmosphere or a secondary stage absorption; ⑨ flue gas analyzer.

Figure 1: Illustration of off-gas treatment unit connected with thermal plasma reactor.

Figure 2: Picture of off-gas treatment unit connected with (a) RF and (b) DC plasma reactor.

3 Results and discussion

3.1 Formation of NO_x in air-plasma

NO_x includes N_2O, NO, NO_2, N_2O_3, N_2O_4, and N_2O_5, in which NO and NO_2 are often referred to as air pollutants. The formation of NO_x can be ruled by the following reactions between N_2 and O_2:

$$N_2 + O_2 \rightarrow 2NO \tag{1}$$

$$N_2 + 2O_2 \rightarrow 2NO_2 \tag{2}$$

$$2N_2 + O_2 \rightarrow 2N_2O \tag{3}$$

$$2N_2 + 3O_2 \rightarrow 2N_2O_3 \tag{4}$$

$$N_2 + 2O_2 \rightarrow N_2O_4 \tag{5}$$

$$2N_2 + 5O_2 \rightarrow 2N_2O_5 \tag{6}$$

Whether a chemical reaction occurs spontaneously is usually judged by the change of the Gibbs free energy ΔG. Thermodynamic calculation has been made based on the data given in the literature [35]. Figure 3 shows ΔG of the above reactions as a function of temperature.

ΔG value for reaction in Eq. 1 decreases as the temperature increases and becomes lower than zero at the temperature around 7,300°C, indicating that reaction in Eq. 1 could take place spontaneously when the temperature is above 7,300°C. ΔG value for other reactions increases as the temperature increases and keeps positive. Thermodynamic calculation shows that the earlier reactions to form NO_x cannot occur under conventional conditions.
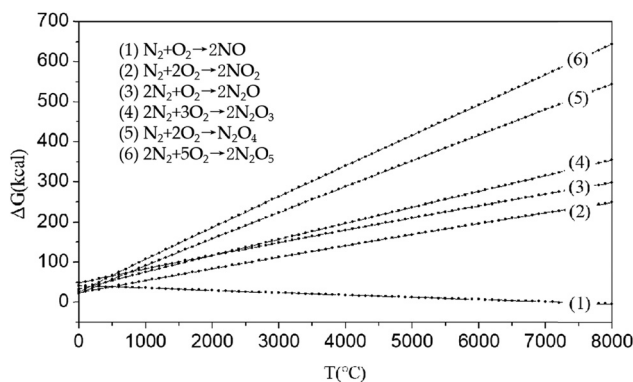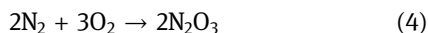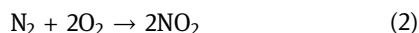

Figure 3: ΔG of the above reactions as a function of temperature.

NO$_x$ in nature mainly originates from lightning, which is a form of plasma. Plasma can provide highly chemically active species, promoting reactions that cannot occur under normal conditions. That is the reason why NO$_x$ can be detected in the off-gas of thermal plasma.

3.2 Detection of NO$_x$ from air-plasma

Detection of NO$_x$ was first conducted using the 50 kW air-plasma. Detailed plasma parameters are listed in Table 1.

Figure 4 shows the NO$_x$ concentration in the off-gas from the 50 kW air-plasma. The concentration increased and reached a stable value 12 s after the beginning of the test. The time lag is because one needs to pump the off-gas into the analyzer for analysis.

The mean concentration was calculated based on the last four data as shown in Table 2. The mean concentration of NO and NO$_2$ was 2,101 and 388 ppm, respectively, and the total NO$_x$ content is 2,489 ppm. The ratio of NO/NO$_2$ after stabilization is about 5.4.

Table 2: NO$_x$ concentration and the calculated mean value

Serial number	NO (ppm)	NO$_2$ (ppm)	NO$_x$ (ppm)
01	2,077	389	2,466
02	2,107	381	2,488
03	2,117	392	2,509
04	2,104	389	2,493
Mean value	2,101	388	2,489
Standard deviation	219.2	16.7	236.5

In order to examine the influence of the plasma power on the NO$_x$ concentration in off-gas, a 150 kW air-plasma was applied. Detailed plasma parameters are listed in Table 3.

Figure 5 shows the NO$_x$ concentration in the off-gas from the 150 kW air-plasma. The air-plasma with the input power of 150 kW was equipped with a plasma wind tunnel, and the detection point was 30 m away from the plasma flame. There was less than 3 m between the plasma flame and detection point when the laboratory had 50 kW plasma. The long distance provided more time for the conversion from NO to NO$_2$ in the air.

Table 1: Detailed parameters for 50 kW air-plasma

Parameters	Values
Rated power	50 kW
Operating voltage	297 V
Operating current	165 A
Total airflow	16 m^3·h^{-1}

Table 3: Detailed parameters for 150 kW air-plasma

Parameters	Values
Rated power	150 kW
Operating voltage	410 V
Operating current	348 A
Total airflow	50 m^3·h^{-1}

Figure 4: NO$_x$ concentration in the off-gas from air-plasma at different sampling times.
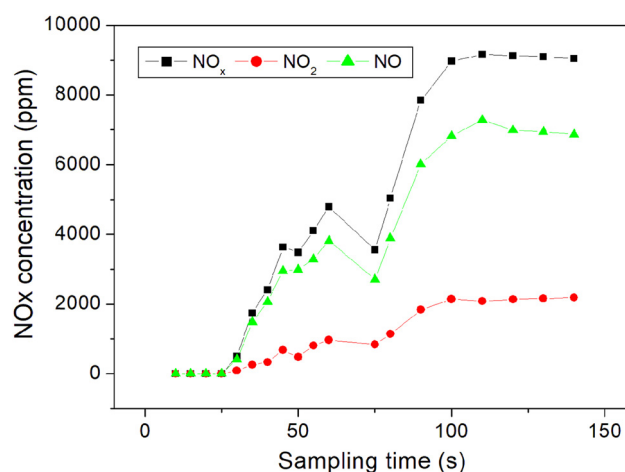

Figure 5: NO$_x$ concentration in the off-gas from air-plasma at different sampling times.

Table 4 shows the NO_x concentration in the off-gas from the air-plasma with the input power of 150 kW. This test was started from the moment when the plasma ignited. It can be seen that the concentration of NO and NO_2 raised from zero and reached a stable value of 100 s after the beginning of the test.

The mean concentration was also calculated based on the last four data provided in Table 4. The mean concentration of NO and NO_2 was 6,968 and 2,143 ppm, respectively, and the total NO_x concentration was 9,112 ppm. The ratio of NO/NO_2 after stabilization was about 3.25. The decrease in NO/NO_2 ratio from 5.4 to 3.25 was related to the detection position.

3.3 Removal of NO_x from air-plasma

3.3.1 Selection of adsorption method

NO_x removal technology mainly includes selective catalytic reduction, selective non-catalytic reduction, solid adsorption method, liquid absorption method, and microbiological method [36]. Among them, the liquid absorption method uses simple equipment to obtain high removal efficiency and large adsorption capacity. According to the type of absorbent and purification principle, the liquid absorption method can be divided into water absorption method, acid absorption method, alkali absorption method, oxidation absorption method, and absorption reduction method [37,38].

At the beginning of this work, the water absorption method was first selected in consideration that water is cheap and pollution-free. Otherwise, it could avoid the corrosive effect of acid and alkali solutions on the equipment. A water circulating pump was used to extract the plasma tail gas and maintain the negative pressure state of the system. The water in the circulating pump also acted as the absorption liquid for NO_x removal. It turned out that the absorption effect was not obvious, because the laboratory was still filled with a pungent smell after water absorption. We terminated the experiment immediately and used alkali absorption method instead.

The alkali solution absorption method uses the alkali solution (NaOH, KOH, or Na_2CO_3) to react with NO_x and generate nitrate and nitrite, so as to remove NO_x. However, the solubility of NO in water and solution is very low, so the alkali solution absorption method is generally only applicable to off-gas with high NO_2 content. The off-gas from thermal air-plasma is typically of high NO content as the testing results in Section 3.2, which does not seem apparently to be suitable for alkali absorption treatment.

Oxidation absorption is a method that oxidizes NO to NO_2 with an oxidant, in order to promote NO_x absorption in an alkali solution. Oxidants mainly include gas-phase oxidants such as O_2, O_3, Cl_2, and ClO_2, and liquid-phase oxidants such as $KMnO_4$, $NaClO_2$, $NaClO$, H_2O_2, HNO_3, and Na_2CrO_4. The reactions can be formulated as follows when O_2 is used as oxidant and NaOH is used in absorption solution:

$$2NO + O_2 \rightarrow 2NO_2 \tag{7}$$

$$2HNO_3 + NaOH \rightarrow NaNO_3 + H_2O \tag{8}$$
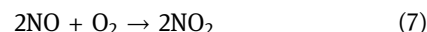
It is gratifying that the off-gas from thermal air-plasma is still mainly composed of O_2 and N_2. In order to determine the O_2 and N_2 content, the off-gas was collected from the plasma reactor using gas bags and characterized by gas chromatography. Table 5 shows the ratio of O_2/N_2 in pure air and the off-gas from air-plasma with the input power of 150 kW. The values are 0.276 and

Table 4: NO_x concentration in the off-gas from air-plasma with the input power of 150 kW

Serial number	Time (s)	NO (ppm)	NO_2 (ppm)	NO_x (ppm)
01	10	0.0	0.0	0.0
02	15	0.0	0.0	0.0
03	20	0.0	0.2	0.2
04	25	0.0	0.0	0.0
05	30	414.0	86.2	500.2
06	35	1,484.0	257.6	1,741.6
07	40	2,068.0	336.1	2,404.1
08	45	2,952.0	680.0	3,632.0
09	50	2,995.0	482.3	3,477.3
10	55	3,289.0	812.1	4,101.1
11	60	3,819.0	971.6	4,790.6
12	75	2,711.0	844.6	3,555.6
13	80	3,890.0	1,142.1	5,032.1
14	90	6,008.0	1,837.5	7,845.5
15	100	6,821.0	2,145.8	8,966.8
16	110	7,084.0	2,083.6	9,167.6
17	120	6,987.0	2,139.3	9,126.3
18	130	6,938.0	2,164.1	9,102.1
19	140	6,866.0	2,186.1	9,052.1

Table 5: Ratio of O_2/N_2 in pure air to the off-gas

Sample	O_2 (vol%)	N_2 (vol%)	Ratio of O_2/N_2
Pure air	21.6	78.4	0.276
Off-gas	20.2	79.8	0.253

0.253, respectively. The atomic ratio of O/N in NO_x (whether 1/1 in NO or 2/1 in NO_2) is greater than that in the air (0.276). The reaction between O_2 and N_2 to form NO_x would consume more O_2 than N_2 and result in a decrease of O_2 and an increase of N_2 content. That is the reason why the off-gas exhibited a lower O_2 content and higher N_2 content than air.

Now that there is O_2 in the off-gas that can act as an oxidant to promote NO absorption, the alkali absorption method can be directly used for treatment of the present off-gas from air-plasma. In consideration that the alkali solution would corrode the water circulating pump, a spray tower (shown in Figure 1) was built.

3.3.2 Effect of gas flow

The concentration of NaOH solution as absorption liquid is 16 wt%. The flow of the liquid pump for NaOH solution circulation was 30 $L \cdot min^{-1}$. The torch power was kept constant, and the off-gas was pumped and introduced into the absorption tower through a branch connected to the exhaust pipeline. The gas flow was regulated by a rotameter from 2.5 to 20.0 $m^3 \cdot h^{-1}$. Figure 6 shows the effect of gas flow on the absorption efficiency.

The absorptivity of NO_x increased obviously from 6.5% to 61.2% when the gas flow decreased from 20 to 2.5 $m^3 \cdot h^{-1}$. The absorptivity of NO also increased from 5.3% to 52.5%. However, the concentration of NO_2 increased instead of decreased and showed an opposite changing trend. The absorptivity of NO_2 was −4.7% with the gas flow of 20 $m^3 \cdot h^{-1}$ and decreased to −16.0% with the gas flow of 2.5 $m^3 \cdot h^{-1}$.
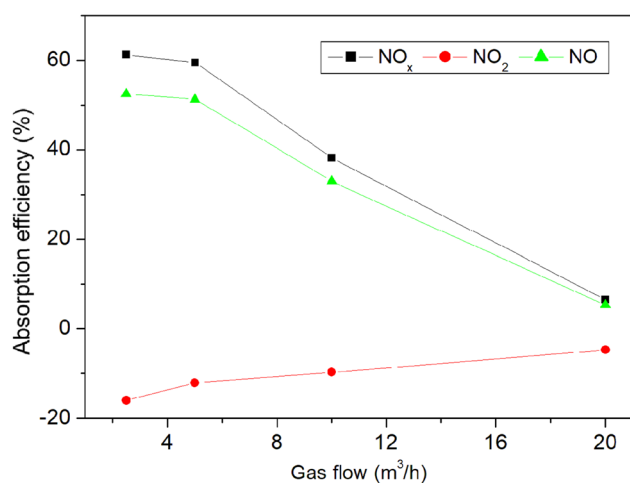
Both the decrease of NO and increase of NO_2 during the absorption process were related to the conversion rate of NO to NO_2. When the gas flow decreased from 20 to 2.5 $m^3 \cdot h^{-1}$, the residence time was prolonged by eight times, which provided more sufficient time for the conversion from NO to NO_2. In order to give a clear explanation, we suppose that the conversion from NO to NO_2 is divided into two stages, before and after absorption. The residence time was prolonged for both stages. At the first stage before absorption, a longer residence time was attributed to the higher conversion from NO to NO_2, resulting in an absorption efficiency, which is the reason why the absorptivity of NO increased obviously with the gas flow decrease. At the second stage after absorption, a longer residence time was still attributed to the higher conversion from NO to NO_2, resulting in an increase in NO_2 concentration.

3.3.3 Effect of O_2 content

It is demonstrated from the above results that O_2 in the off-gas must have played an important role so that alkali absorption method can be directly used for the treatment of the off-gas from air-plasma with high NO content. Inspired by this O_2-enhanced absorption process, we provided additional O_2 into the off-gas to increase its O_2 content. Figure 7 shows the absorption efficiency with and without additional O_2. The O_2 flow was 1.5 $m^3 \cdot h^{-1}$ when the off-gas was 2.5 $m^3 \cdot h^{-1}$. The concentration of O_2 was increased from about 20% to about 50%. The absorptivity of NO increased slightly from 61.2% to 69.7%, while the absorptivity of NO_2 increased obviously from −16% to 16%. The obvious increase in NO_2 absorptivity cannot be explained clearly through the change of residence time.
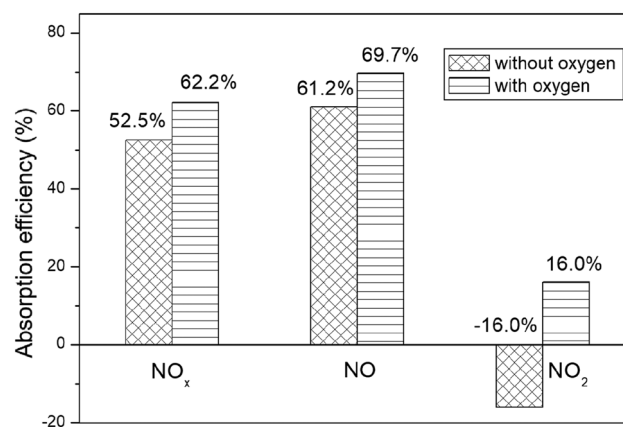

Figure 6: Effect of gas flow on the absorption efficiency.

Figure 7: The absorption efficiency with and without additional O_2.

It indicated that O_2 might have played a synergistic absorption role except that it can convert NO to NO_2 as an oxidant during different stages. The total NO_x absorptivity increased from 52.5% to 62.2%.

3.3.4 Design of multistage unit

Taking the gas flow and O_2 content effects into account, the content of NO and NO_2 was reduced to a fairly low level at 436 and 197.2 ppm, respectively. The total content of NO_x was 633.2 ppm, which has not reached the emission standard of 200 ppm. Multistage absorption is a commonly used strategy in industrial production to increase absorption efficiency.

The number of cycles of absorption can be estimated from the absorption rate. In the above absorption experiment, the initial concentration of NO_x was 1,674.9 ppm, and the concentration after one cycle absorption was 633.2 ppm. The absorption rate was 62.2%. The NO_x concentration was detected at different positions as shown in Figure 8: the inlet of the first absorption tower, the outlet of the first absorption tower, the outlet of the second absorption tower, and the outlet of the third absorption tower. The NO_x concentration and the absorption rate after different cycles of absorption were estimated, and the results are shown in Table 6.

It can be estimated that NO_x concentration after a three-cycle absorption can be reduced below 100 ppm which can meet the emission standard. Based on the assessment, we have designed a multistage unit for the treatment of off-gas from air plasma, as shown in Figure 8.

Table 6: Estimated concentration of NO_x after different cycles of absorption

Cycle number	Cumulative absorption rate (%)	NO_x concentration (ppm)
0	0	1,674.9
1	62.2	633.2
2	85.7	239.2
3	94.6	90.5

This article intends to present the feasibility of thermal plasma off-gas purification. Further testing and application according to detailed plasma running parameters are still in progress.

4 Conclusions

The concentration of NO_x in off-gas from air-plasma was determined by a gas analyzer, removal methods were selected according to the characteristics of plasma off-gas, different influencing parameters were examined, and a treatment unit was designed for the green air-plasma process. Several conclusions can be drawn from the results and discussion:

1. N_2 and O_2 would react and form NO_x in the unordinary chemical reaction media provided by thermal plasma, and the concentration of NO_x in off-gas from air-plasma increased with the increase in plasma power.
2. The content of O_2 in the off-gas was close to that in air, which would act as an oxidant to promote NO_x
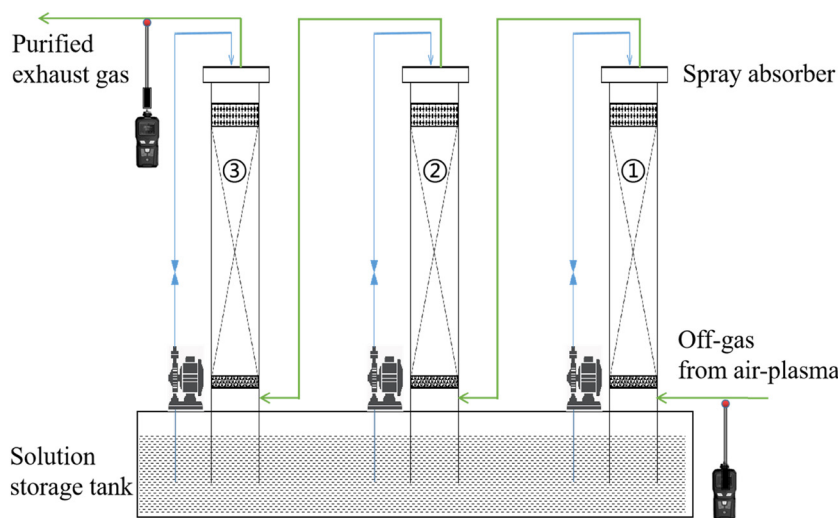

Figure 8: Illustration of a multistage off-gas treatment unit.

absorption; thus, alkali absorption method can be directly used for the treatment of the present off-gas from air-plasma.

3. The absorption efficiency was 52.5% when the gas flow was $2.5\,m^3{\cdot}h^{-1}$, and it could be further increased to 62.2% when additional O_2 was provided into the off-gas to increase its O_2 content from 20% to 50%.

4. It was estimated that the NO_x concentration can be reduced below 100 ppm when a multistage absorption unit was designed, which can meet the emission standard and present a feasible technical scheme for the green plasma process.

Author contributions: Liuyang Bai: conceptualization, methodology, investigation, writing – original draft preparation, writing – review and editing, project administration, funding acquisition; Yuge Ouyang: methodology, writing – original draft preparation, writing – review and editing; Hongbing Wang: investigation, visualization; Min Wang: investigation, visualization; Fangli Yuan: conceptualization, supervision, funding acquisition. All authors have read and agreed to the published version of the manuscript.

Conflict of interest: The authors state no conflict of interest.

References

[1] Boulos MI, Fauchais P, Pfender E. Thermal plasmas: Fundamentals and applications. New York: Plenum Press; 1994.

[2] Sikarwar VS, Hrabovský M, Van OG, Pohořelý M, Jeremiáš M. Progress in waste utilization via thermal plasma. Prog Energy Combust Sci. 2020;81:100873. doi: 10.1016/j.pecs.2020.100873.

[3] Prado ES, Miranda FS, de Araujo LG, Petraconi G, Baldan MR. Thermal Plasma Technology for radioactive waste treatment: A Review. J Radioanal Nucl Chem. 2020;325(2):331–42. doi: 10.1007/s10967-020-07269-4.

[4] Schumacher U. Basics of plasma physics. In: Dinklage A, Klinger T, Marx G, Schweikhard L, (eds). Plasma Physics. Lecture Notes in Physics. Berlin, Heidelberg: Springer; 2005. doi: 10.1007/11360360_1.

[5] Petitpas G, Rollier J, Darmon A. A comparative study of non-thermal plasma assisted Reforming Technologies. Int J Hydrog Energ. 2007;32(14):2848–67. doi: 10.1016/j.ijhydene.2007.03.026.

[6] Huang H, Tang L. Treatment of organic waste using thermal plasma pyrolysis technology. Energy Convers Manag. 2007;48:1331–7. doi: 10.1016/j.enconman.2006.08.013.

[7] Chen FF. Introduction to plasma physics. New York: Springer Science & Business Media; 1974.

[8] Zhukov MF, Zasypkin IM, Timoshevskii AN. Thermal plasma torches: design, characteristics, application. Cambridge: Cambridge International Science Publishing; 2007.

[9] Yuan FL, Jin HC, Hou GL. Progress on preparation of special powders using HF thermal plasma (in Chinese). Chin J Process Eng. 2018;18(6):1139–45. doi: 10.12034/j.issn.1009-606X.218240.

[10] Zheng J, Yang R, Xie L, Qu J, Liu Y, Li X. Plasma-assisted approaches in inorganic nanostructure fabrication. Adv Mater. 2010;22(13):1451–73. doi: 10.1002/adma.200903147.

[11] He J, Bai L, Jin H, Yuan F. Optimization of tungsten particles spheroidization with different size in thermal plasma reactor based on numerical simulation. Powder Technol. 2016;302:288–97. doi: 10.1016/j.powtec.2016.08.067.

[12] Zhu H, Li X, Chen Q. Three-dimensional simulation and experimental investigation on spheroidization of stainless steel powders using radio frequency thermal plasma. J Mater Eng Perform. 2022;31:6606–16. doi: 10.1007/s11665-022-06714-7.

[13] Hu P, Yan S, Yuan F, Bai L, Li J, Chen Y. Effect of plasma spheroidization process on the microstructure and crystallographic phases of silica, alumina and nickel particles. Plasma Sci Technol. 2007;9(5):611–5. doi: 10.1088/1009-0630/9/5/20.

[14] He J, Bai L, Jin H, Jia Z, Hou G, Yuan F. Simulation and experimental observation of silicon particles' vaporization in RF thermal plasma reactor for preparing si nano-powder. Powder Technol. 2017;313:27–35. doi: 10.1016/j.powtec.2017.02.062.

[15] Bai L, He J, Ouyang Y, Liu W, Liu H, Yao H, et al. Modeling and selection of RF thermal plasma hot-wall torch for large-scale production of nanopowders. Materials. 2019;12(13):2141. doi: 10.3390/ma12132141.

[16] Hou G, Cheng B, Ding F, Yao M, Cao Y, Hu P, et al. Well dispersed silicon nanospheres synthesized by RF thermal plasma treatment and their high thermal conductivity and dielectric constant in polymer nanocomposites. RSC Adv. 2015;5(13):9432–40. doi: 10.1039/c4ra14212h.

[17] Bai L, Yuan F, Fang Z, Wang Q, Ouyang Y, Jin H, et al. RF thermal plasma synthesis of ultrafine ZrB₂-ZrC composite powders. Nanomaterials. 2020;10(12):2497. doi: 10.3390/nano10122497.

[18] Bai L, Fan J, Hu P, Yuan F, Li J, Tang Q. RF plasma synthesis of nickel nanopowders via hydrogen reduction of nickel hydroxide/carbonate. J Alloy Compd. 2009;481(1–2):563–7. doi: 10.1016/j.jallcom.2009.03.054.

[19] Zhang H, Yao M, Bai L, Xiang W, Jin H, Li J, et al. Synthesis of uniform octahedral tungsten trioxide by RF induction thermal plasma and its application in gas sensing. CrystEngComm. 2013;15(7):1432. doi: 10.1039/c2ce26514a.

[20] Zhang X, Wang Y, Min BI, Kumai E, Tanaka M, Watanabe T. A controllable and byproduct-free synthesis method of carbon-coated silicon nanoparticles by induction thermal plasma for Lithium Ion Battery. Adv Powder Technol. 2021;32(8):2828–38. doi: 10.1016/j.apt.2021.06.003.

[21] Yang Z, Du Y, Yang Y, Jin H, Shi H, Bai L, et al. Large-scale production of highly stable silicon monoxide nanowires by radio-frequency thermal plasma as anodes for high-performance Li-Ion Batteries. J Power Sources. 2021;497:229906. doi: 10.1016/j.jpowsour.2021.229906.

[22] Li X, Xin W, Zheng X, Ren Z, Sun D, Lu W. Microstructural characterization and formation mechanism of nitrided layers on aluminum substrates by thermal plasma nitriding. Metals. 2019;9(5):523. doi: 10.3390/met9050523.

[23] Rajendran I, Shreeram B. Corrosion, adhesion and erosion study of MZ and ML system using thermal plasma. Int J Heavy Veh Syst. 2018;25(3/4):406. doi: 10.1504/ijhvs.2018.10016136.

[24] Moustakas K, Fatta D, Malamis S, Haralambous K, Loizidou M. Demonstration plasma gasification/vitrification system for effective hazardous waste treatment. J Hazard Mater. 2005;123(1–3):120–6. doi: 10.1016/j.jhazmat.2005.03.038.

[25] Cheng TW, Tu CC, Ko MS, Ueng TH. Production of glass–ceramics from incinerator ash using lab-scale and pilot-scale thermal plasma systems. Ceram Int. 2011;37(7):2437–44. doi: 10.1016/j.ceramint.2011.05.088.

[26] Károly Z, Mohai I, Tóth M, Wéber F, Szépvölgyi J. Production of glass–ceramics from fly ash using Arc Plasma. J Eur Ceram Soc. 2007;27(2–3):1721–5. doi: 10.1016/j.jeurceramsoc.2006.05.015.

[27] Morrin S, Lettieri P, Chapman C, Mazzei L. Two stage fluid bed-plasma gasification process for solid waste valorisation: technical review and preliminary thermodynamic modelling

of sulphur emissions. Waste Manag. 2012;32:676–84. doi: 10.1016/j.wasman.2011.08.020.

[28] Fabry F, Rehmet C, Rohani V, Fulcheri L. Waste gasification by thermal plasma: a review. Waste Biomass Valor. 2013;4(421):439. doi: 10.1007/s12649-013-9201-7.

[29] Sanlisoy A, Carpinlioglu MO. A review on plasma gasifcation for solid waste disposal. Int J Hydrog Energy. 2017;42:1361–5. doi: 10.1016/j.ijhydene.2016.06.008.

[30] Changming D, Chao S, Gong X. Plasma methods for metals recovery from metal-containing waste. Waste Manag. 2018;77:373–87. doi: 10.1016/j.wasman.2018.04.026.

[31] Bai L, Sun W, Yang Z, Ouyang Y, Wang M, Yuan F. Laboratory research on design of three-phase AC arc plasma pyrolysis device for recycling of waste printed circuit boards. Processes. 2022;10(5):1031. doi: 10.3390/pr10051031.

[32] Abdulkarim BI, Hassan MAA. Thermal plasma treatment of wastes: a review. Aust J Basic Appl Sci. 2015;9(31):322–33.

[33] Hrabovský M. Generation of thermal plasmas in liquid-stabilized and hybrid DC-arc torches. Pure Appl Chem. 2002;74(3):429–33. doi: 10.1351/pac200274030429.

[34] Watanabe T, Shimbara S. Halogenated hydrocarbon decomposition by steam thermal plasmas. High Temp Mater Process. 2003;7(4):455–74. doi: 10.1615/hightempmatproc.v7.i4.30.

[35] Knacke O, Kubaschewski O, Hesselmann K. Thermochemical properties of inorganic substances. Berlin/NewYork; Verlag Stahleisen, Dsseldorf: Springer-Verlag; 1991.

[36] Wang D, Li S, Yang S, Ji L. Current status and prospects of the application of industrial denitration technology. Sci Technol Chem Indus. 2020;28(2):77–82.

[37] Si M, Shen B, Adwek G, Xiong L, Liu L, Yuan P, et al. Review on the NO removal from flue gas by oxidation methods. J Env Sci. 2021;101:49–71. doi: 10.1016/j.jes.2020.08.004.